

Fig. 9.2 Part a) shows the disconnected contribution given by Eq. (9.44) contributing to the first-order  $\hat{U}$  term in Eq. (9.17). Part b) represents the graphical representation of the other contribution given by Eq. (9.45). Note that the three times indicated by arrows are not time-ordered. This means that all allowed time-orderings are contained in these types of diagrams, usually referred to as Feynman diagrams.

a graphical representation shown in Fig. 9.2 with corresponding analytical expressions

$$U_I \Rightarrow \left\{ \int_{-\infty(1-i\eta)}^{\infty(1-i\eta)} dt_1 \sum_{\gamma\delta} \langle \gamma | U | \delta \rangle G^{(0)}(\delta, \gamma; t_1 - t_1^+) \right\} G^{(0)}(\alpha, \beta; t-t') \quad (9.44)$$

and

$$U_{II} \Rightarrow - \int_{-\infty(1-i\eta)}^{\infty(1-i\eta)} dt_1 \sum_{\gamma\delta} \langle \gamma | U | \delta \rangle G^{(0)}(\alpha, \gamma; t - t_1) G^{(0)}(\delta, \beta; t_1 - t'). \quad (9.45)$$

It is important to realize that the time-orderings in these diagrams are not fixed. For this reason these types of diagrams are referred to as Feynman diagrams. In drawing diagrams contributing to the sp propagator in the time formulation it is important to keep in mind that both time-orderings  $t > t'$  and  $t' > t$  are represented by the same diagram. In addition, the internal time integrations range over all times so that in the case of Fig. 9.2  $t_1$  can be in any position relative to  $t$  and  $t'$ . By separating all these different cases it is possible to generate all time-ordered diagrams for this contribution. One such example is given by Fig. 9.1. In most cases the efficiency of the Feynman diagram formulation is preferable over the more cumbersome time-ordered result.

The treatment of the first-order term in the numerator of Eq. (9.17) involving the two-body interaction term  $\hat{V}$  involves a time-ordered product of three particle addition and three removal operators and therefore generates  $3!$  terms each containing three noninteracting propagators. This results in

the following expression for this contribution

$$\begin{aligned}
\hat{V}^{n=1} \Rightarrow & i\hbar \int_{-\infty(1-i\eta)}^{\infty(1-i\eta)} dt_1 \frac{1}{2} \sum_{\gamma\delta\epsilon\theta} (\gamma\delta|V|\epsilon\theta) \\
& \times \left\{ G^{(0)}(\alpha, \beta; t-t') \left[ \underbrace{G^{(0)}(\theta, \delta; t_1-t_1^+) G^{(0)}(\epsilon, \gamma; t_1-t_1^+)}_I \right. \right. \\
& \quad \left. \left. - \underbrace{G^{(0)}(\theta, \gamma; t_1-t_1^+) G^{(0)}(\epsilon, \delta; t_1-t_1^+)}_{II} \right] \right. \\
& + G^{(0)}(\alpha, \gamma; t-t_1) \left[ \underbrace{G^{(0)}(\theta, \beta; t_1-t') G^{(0)}(\epsilon, \delta; t_1-t_1^+)}_{IV} \right. \\
& \quad \left. - \underbrace{G^{(0)}(\theta, \delta; t_1-t_1^+) G^{(0)}(\epsilon, \beta; t_1-t')}_{III} \right] \\
& + G^{(0)}(\alpha, \delta; t-t_1) \left[ \underbrace{G^{(0)}(\theta, \gamma; t_1-t_1^+) G^{(0)}(\epsilon, \beta; t_1-t')}_{VI} \right. \\
& \quad \left. - \underbrace{G^{(0)}(\theta, \beta; t_1-t') G^{(0)}(\epsilon, \gamma; t_1-t_1^+)}_V \right] \left. \right\}. \quad (9.46)
\end{aligned}$$

These six terms may be graphically represented as shown in Fig. 9.3. As the topology suggests, diagrams *III* and *V* are identical as are *IV* and *VI*. This can be verified by exchanging dummy summation variables and using the property of Eq. (2.43). It is customary then to consider only diagrams *III* and *IV* and multiply the corresponding expressions by a factor of 2. The first two diagrams are of the disconnected kind as the one representing Eq. (9.44) shown in part *a*) of Fig. 9.2. These diagrams cancel corresponding terms in the denominator of Eq. (9.17). Anticipating this result, the first-order contribution to the propagator then becomes

$$\begin{aligned}
G^{(1)}(\alpha, \beta; t-t') = & - \int dt_1 \sum_{\gamma\delta} \langle \gamma|U|\delta \rangle G^{(0)}(\alpha, \gamma; t-t_1) G^{(0)}(\delta, \beta; t_1-t') \\
& - i\hbar \int dt_1 \sum_{\gamma\delta\epsilon\theta} (\gamma\delta|V|\epsilon\theta) \\
& \times \left\{ G^{(0)}(\alpha, \gamma; t-t_1) G^{(0)}(\theta, \delta; t_1-t_1^+) G^{(0)}(\epsilon, \beta; t_1-t') \right. \\
& \quad \left. - G^{(0)}(\alpha, \gamma; t-t_1) G^{(0)}(\epsilon, \delta; t_1-t_1^+) G^{(0)}(\theta, \beta; t_1-t') \right\}. \quad (9.47)
\end{aligned}$$

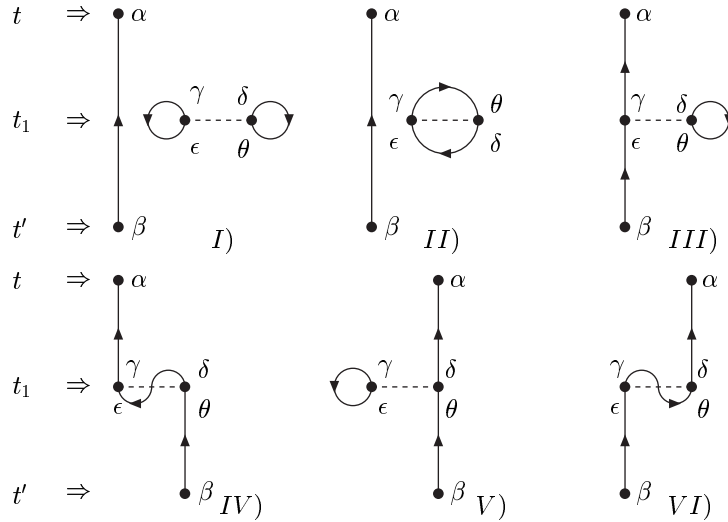


Fig. 9.3 Six diagrams corresponding to the six terms in Eq. (9.46). Note that diagrams *I* and *II* are of the disconnected kind and will be canceled by corresponding contribution from the numerator of Eq. (9.17).

It should be noted that the time integration limits has been suppressed in this expression. This first-order correction to the propagator therefore includes diagram *b* from Fig. 9.2 and diagrams *III* and *IV* from Fig. 9.3 as is the custom. It is quite often useful to reduce the number of diagrams even further by combining the matrix elements of the two-body interaction  $\hat{V}$  as in Eq. (2.47). The resulting contribution from the two-body interaction to  $G^{(1)}$  can then be written as

$$G_{\hat{V}}^{(1)}(\alpha, \beta; t - t') = -i\hbar \int dt_1 \sum_{\gamma\delta\epsilon\theta} \langle \gamma\delta | V | \epsilon\theta \rangle \times G^{(0)}(\alpha, \gamma; t - t_1)G^{(0)}(\theta, \delta; t_1 - t_1^+)G^{(0)}(\epsilon, \beta; t_1 - t'). \tag{9.48}$$

For systems that have comparable contributions for the direct and exchange contribution in Eq. (2.47) this strategy is particularly useful. If it is adopted, only diagram *III* in Fig. 9.3 will have to be considered in first order in  $\hat{V}$ . The labeling of the interactions which is represented by a dashed line in Fig. 9.3 is usually done by reserving the two top locations for the final two-particle state and the two bottom ones for the initial state. To avoid contorting diagram *II* this convention is not applied in that case. No ambiguity should arise, however, since one can identify initial and

final states by the directions of the arrows associated with the attached propagators.

The cancellation of the factor of  $1/2$  through the appearance of equivalent diagrams also occurs in higher order. In addition, for any diagram in higher order there is an identical contribution from topologically equivalent diagrams that differ only in the permutation of the time labels  $t_1, t_2, \dots, t_n$  since one can move the  $\hat{H}_1(t_i)$  at will under the  $\mathcal{T}$  sign. Since there are  $n!$  such terms this generates a factor of  $n!$  which cancels the  $1/n!$  term in the numerator of Eq. (9.17).

We now turn our attention to the denominator of Eq. (9.17) to clarify the mechanism of the cancellation alluded to above. This denominator is sometimes denoted by

$$\langle \Phi_0^A | \hat{S} | \Phi_0^A \rangle = \sum_m \left( \frac{-i}{\hbar} \right)^m \frac{1}{m!} \int dt'_1 \dots \int dt'_m \langle \Phi_0^A | \mathcal{T} [\hat{H}_1(t'_1) \dots \hat{H}_1(t'_m)] | \Phi_0^A \rangle. \quad (9.49)$$

When considering contributions to Eq (9.49) one can proceed in a similar fashion in generating a diagrammatic representation for each order  $m$ . Clearly for  $m = 0$  this contribution is 1. By direct application of Wick's theorem the first-order term yields

$$\begin{aligned} \langle \Phi_0^A | \hat{S}^{(1)} | \Phi_0^A \rangle &= \int dt_1 \sum_{\gamma\delta} \langle \gamma | U | \delta \rangle G^{(0)}(\delta, \gamma; t_1^+ - t_1) \\ &\quad - i\hbar \int dt_1 \frac{1}{2} \sum_{\gamma\delta\epsilon\theta} (\gamma\delta | V | \epsilon\theta) \left\{ G^{(0)}(\theta, \delta; t_1 - t_1^+) G^{(0)}(\epsilon, \gamma; t_1 - t_1^+) \right. \\ &\quad \left. - G^{(0)}(\theta, \gamma; t_1 - t_1^+) G^{(0)}(\epsilon, \delta; t_1 - t_1^+) \right\}. \quad (9.50) \end{aligned}$$

The numerator of Eq. (9.17) contains a contribution in first order of the type  $G^{(0)} \times \langle \Phi_0^A | \hat{S}^{(1)} | \Phi_0^A \rangle$  as can be verified from the results of Eqs. (9.44) and (9.46). Taking the corresponding lowest order contribution to the numerators and denominator of Eq. (9.17) into account, one can therefore write schematically

$$\begin{aligned} G(\alpha, \beta; t - t') &= \left\{ G^{(0)}(\alpha, \beta; t - t') \times (1 + \langle \Phi_0^A | \hat{S}^{(1)} | \Phi_0^A \rangle + \dots) \right. \\ &\quad \left. + G^{(1)}(\alpha, \beta; t - t') \times (1 + \dots) + \dots \right\} \\ &\quad / \left\{ 1 + \langle \Phi_0^A | \hat{S}^{(1)} | \Phi_0^A \rangle + \dots \right\}. \quad (9.51) \end{aligned}$$

One may recognize the incipient cancellation that will occur between the

numerator and denominator of Eq. (9.51). When analyzing higher-order contributions, one always encounters connected terms, linked to both  $a_\alpha(t)$  and  $a_\beta^\dagger(t')$ , possibly multiplied by disconnected ones leading to a factorized contribution to the numerator of Eq. (9.17). This implies that in  $n$ th one is able to write for this numerator contribution [Abrikosov *et al.* (1975)]

$$\begin{aligned} G_{\text{numerator}}^{(n)}(\alpha, \beta; t - t') &= -\frac{i}{\hbar} \sum_l \sum_m \left(\frac{-i}{\hbar}\right)^{l+m} \delta_{n, l+m} \frac{1}{n!} \frac{n!}{l!m!} \\ &\times \int dt_1 \dots \int dt_m \langle \Phi_0^A | \mathcal{T} [\hat{H}_1(t_1) \dots \hat{H}_1(t_m) a_\alpha(t) a_\beta^\dagger(t')] | \Phi_0^A \rangle_{\text{connected}} \\ &\times \int dt_{m+1} \dots \int dt_n \langle \Phi_0^A | \mathcal{T} [\hat{H}_1(t_{m+1}) \dots \hat{H}_1(t_n)] | \Phi_0^A \rangle. \end{aligned} \quad (9.52)$$

One may verify this result by applying Wick's theorem to both sides of this expression. The second part of this result may contain many disconnected parts. The factor  $n!/l!m!$  in Eq. (9.52) represents the number of ways one can distribute the  $n$   $\hat{H}_1$  operators into the two groups. To obtain the complete numerator one simply has to perform the sum over  $n$  which yields

$$\begin{aligned} G_{\text{numerator}}(\alpha, \beta; t - t') &= -\frac{i}{\hbar} \sum_m \left(\frac{-i}{\hbar}\right)^m \frac{1}{m!} \\ &\times \int dt_1 \dots \int dt_m \langle \Phi_0^A | \mathcal{T} [\hat{H}_1(t_1) \dots \hat{H}_1(t_m) a_\alpha(t) a_\beta^\dagger(t')] | \Phi_0^A \rangle_{\text{connected}} \\ &\times \sum_l \left(\frac{-i}{\hbar}\right)^l \frac{1}{l!} \int dt'_1 \dots \int dt'_l \langle \Phi_0^A | \mathcal{T} [\hat{H}_1(t'_1) \dots \hat{H}_1(t'_l)] | \Phi_0^A \rangle. \end{aligned} \quad (9.53)$$

One may now identify the denominator of Eq. (9.17) as the second term in this expression. One therefore obtains the important result that only connected diagrams appear in the expansion for the sp propagator. This cancellation then yields the final expansion of the sp propagator in terms that can, in principle, be calculated order by order from the noninteracting propagator and the interaction Hamiltonian  $\hat{H}_1$

$$\begin{aligned} G(\alpha, \beta; t - t') &= -\frac{i}{\hbar} \sum_m \left(\frac{-i}{\hbar}\right)^m \frac{1}{m!} \int dt_1 \dots \int dt_m \\ &\times \langle \Phi_0^A | \mathcal{T} [\hat{H}_1(t_1) \dots \hat{H}_1(t_m) a_\alpha(t) a_\beta^\dagger(t')] | \Phi_0^A \rangle_{\text{connected}}. \end{aligned} \quad (9.54)$$

Only contributions to the sp propagator that are completely linked and connect to the operators  $a_\alpha(t)$  and  $a_\beta^\dagger(t')$  need to be considered in this

expansion. As indicated above, each contribution to Eq. (9.54) can uniquely associated with a Feynman diagram.

### 9.5 Diagram rules

With the result from Eq. (9.54) and Wick's theorem it is now possible to study the contributions to the sp propagator in a systematic way. The expansion can be fruitfully depicted in a graphical manner accompanied by a small set of rules that allow the construction of the relevant expressions from the diagrams.

#### 9.5.1 Time-dependent version

In the present time-dependent formulation of the expansion one may first consider the rules in the absence of an auxiliary potential  $\hat{U}$ . In that case only diagrams involving the two-body interaction  $\hat{V}$  are encountered. The following rules apply for an the  $m$ th order contribution in this case.

**Rule 1** Draw all topologically distinct and connected diagrams with  $m$  horizontal interaction lines for  $V$  (dashed) and  $2m + 1$  directed (using arrows) Green's functions  $G^{(0)}$

**Rule 2** Label external points appropriately. For example, the labels  $\alpha, t$  and  $\beta, t'$  apply in the present case. Label each interaction with a time and sp quantum numbers

$$t \Rightarrow \begin{array}{c} \gamma \\ \bullet \text{---} \bullet \\ \epsilon \quad \theta \end{array} \Rightarrow (\gamma\delta|V|\epsilon\theta)$$

For each full line one writes

$$\begin{array}{c} t_i \Rightarrow \bullet \mu \\ \updownarrow \\ t_j \Rightarrow \bullet \nu \end{array} \Rightarrow G^{(0)}(\mu, \nu; t_i - t_j)$$

**Rule 3** Sum (integrate) over all internal sp quantum numbers and integrate over all  $m$  internal times

**Rule 4** Include a factor  $(i/\hbar)^m$  and  $(-1)^F$  where  $F$  is the number of closed fermion loops

**Rule 5** Interpret equal times in a propagator as  $G^{(0)}(\mu, \nu; t - t^+)$

If it is unclear whether diagrams are topologically distinct, one can always resort to a direct application of Wick’s theorem. It should be noted that fermion lines either close on themselves yielding a closed loop, or run continuously from the external label  $\alpha$  to the external label  $\beta$ . The closing of a fermion line generates a minus sign since for such a case one can reorder the corresponding contractions without changing the sign into (using symbolic notation)

$$a^\dagger(t_1) \bullet a(t_1) \bullet \bullet a^\dagger(t_2) \bullet \bullet a(t_2)^\circ \dots a^\dagger(t_m)^\circ \circ a(t_m) \bullet \quad (9.55)$$

and one additional sign change is needed to contract the outermost operators according to the convention. The factor  $1/2$  appearing in the second quantized form of  $\hat{V}$  can be discarded provided only diagrams of the type *III* and *IV* are included for Fig. 9.3 and those of type *V* and *VI* are discarded. Similar considerations apply in higher order. The factor  $(i\hbar)^m$  in **Rule 3** results from the prefactor  $-i/\hbar$  in Eq. (9.54), the factor  $(-i/\hbar)^m$  appearing there under the sum, and, finally, a factor  $(i\hbar)^{2m+1}$  from the number of contractions in  $m$ th order. This latter number corresponds to each interaction contributing two contractions plus one extra corresponding to the external operators.

The first-order contributions generated by applying these rules are displayed in Figs. 9.4 and 9.5. The diagram shown in Fig. 9.4 will be labeled “V1D” for the first-order “direct” contribution from  $V$  to the propagator. The exchange diagram in first-order is accordingly labeled “V1E” and shown in Fig. 9.5. In the literature one encounters different ways of drawing

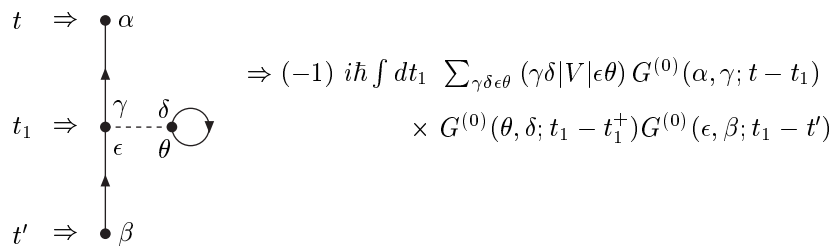


Fig. 9.4 Diagram V1D representing the first-order “direct” contribution from the two-body interaction  $V$  to the sp propagator in the time formulation. The minus sign in front comes from the closed fermion loop.

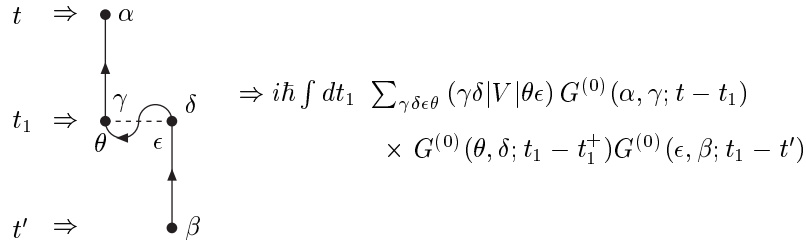


Fig. 9.5 Diagram V1E representing the first-order “exchange” contribution from the two-body interaction  $V$ .

this exchange diagram. Here, the choice has been made to identify clearly how the propagators enter and leave the two-body interaction  $V$ . In addition, it should be noted that all two-body interaction are drawn horizontally to emphasize that most interactions considered in the many-particle problem are static, *i.e.* occur at one time. It is natural to generate nonstatic interaction terms between particles by considering higher-order contributions to the interaction between the particles in the medium. Examples of such interactions will be considered in Ch. 14. For now, it appears more appropriate to reflect the reality of static interactions in drawing diagrams and not use the field-theory version where the interaction lines actually represent bosons that can also propagate allowing for nonstatic interactions. The latter choice of diagrammatic representation was *e.g.* made by [Fetter and Walecka (1971)]. All diagrams up to second order in  $V$  are shown in Figs. 9.6 to 9.15 together with the corresponding expressions obtained from the diagram rules. These diagrams clearly separate into different categories. The first four, shown in Figs. 9.6 to 9.9, are simply repeats of the first-order contributions displayed in Figs. 9.4 and 9.5. All these four diagrams will be categorized as reducible in Ch. 10 since they can be obtained by iterating lower-order contributions. For future reference these diagrams will be labeled  $V2a$  through  $V2d$ .

The next four contributions in second order can also be obtained from each other under exchange. These diagrams are labeled  $V2e$  through  $V2h$  and are shown in Figs. 9.10 - 9.13. These terms are also related to the first-order contributions like diagrams  $V2a$  through  $V2d$  but are obtained by replacing the propagator that leaves from and returns to  $V$  (implying equal time arguments) in the first-order diagrams by the corresponding  $G^{(1)}$  terms represented by diagrams  $V1D$  and  $V1E$  shown in Figs. 9.4 and

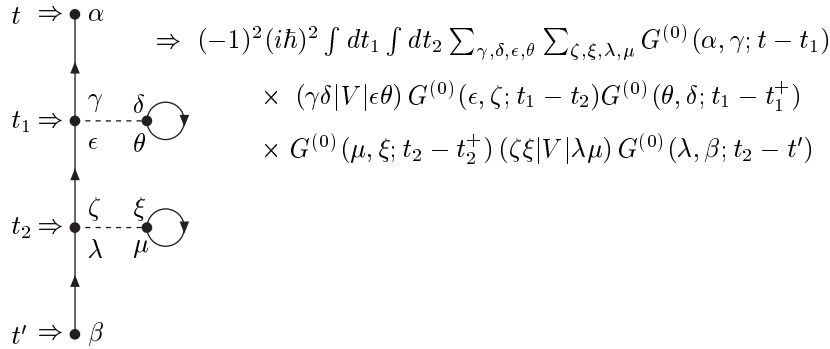


Fig. 9.6 Diagram V2a representing one of the ten second-order contributions to the sp propagator in the time formulation.

9.5, respectively. Especially for some of these four diagrams the topological equivalence with the corresponding terms drawn according to the field-theory convention (see Fig. 9.8 in [Fetter and Walecka (1971)]) may not be immediately obvious. Nevertheless, the present convention clearly emphasizing the static feature of the interaction  $V$ , may be helpful in visualizing the successive dressing of internal propagators that will be further explored in Ch. 10.

The final two diagrams representing second-order contributions are shown in Figs. 9.14 and 9.15. They are labeled by  $V2i$  and  $V2j$ , respec-

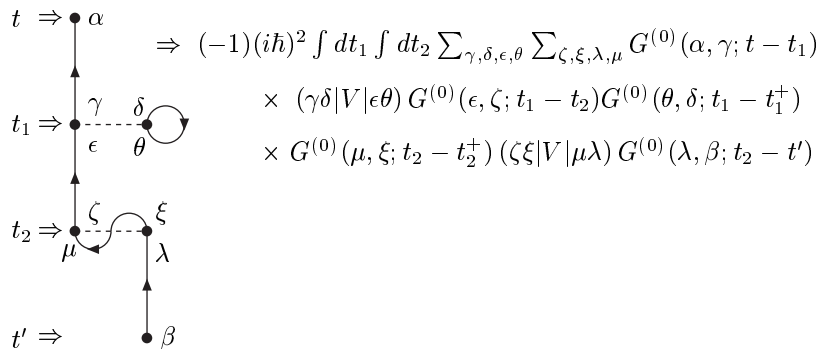


Fig. 9.7 Diagram V2b

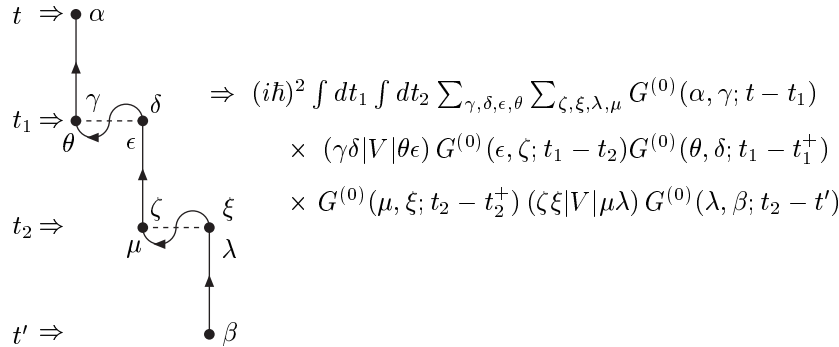


Fig. 9.8 Diagram V2c

tively, and are also related to each other by the exchange operation. Note that there are only two such terms which can be checked explicitly by applying the relevant algebra of Wick's theorem and using the appropriate relabeling of dummy indices. It will be shown in Ch. 13 that the inclusion of these types of diagrams in the propagator will cross the boundary of the central-field or mean-field description. All eight terms represented by Figs. 9.6 to 9.13 (and more) are included in this mean-field description to be discussed in considerable detail in Ch. 11.

Third and higher order contributions can be obtained in a similar fashion. The reader should realize, however, that in practice there is usually

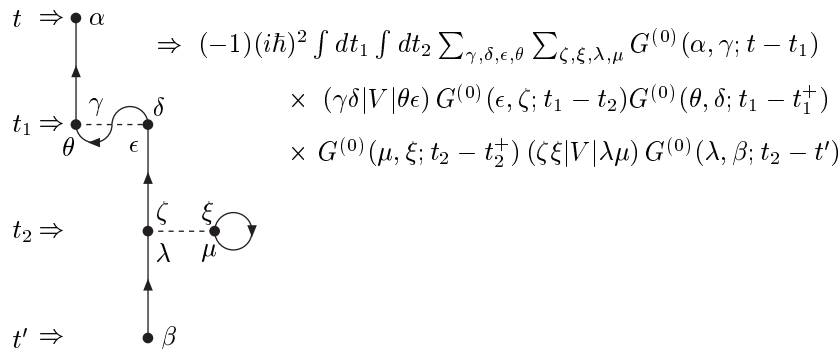


Fig. 9.9 Diagram V2d

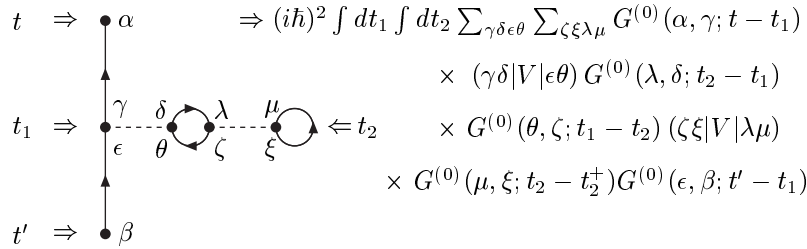


Fig. 9.10 Diagram V2e

never the need to consider such higher-order terms individually unless they are part of infinite sums of diagrams. Nevertheless, it is useful practice to draw examples of higher-order diagrams as will be suggested in the exercises belonging to this chapter. It should also be noted that having obtained the possibility to write down every term in the expansion of the sp propagator, it is by no means clear how to proceed making relevant approximations for a particular system under study. In fact, it will be shown in Ch. 10 that one requires infinite summations of diagrams to obtain sensible results even if the two-body interaction is quite weak.

Sofar only terms involving the two-body interactions have been discussed. While these terms determine the general structure of the diagrams, it is sometimes necessary to introduce the auxiliary potential  $\hat{U}$  as in Eq. (9.20). In this situation one has to include additional diagrams and corresponding rules to deal with the contributions of this one-body interaction term in the perturbation expansion. In first order, the corresponding diagram is shown in Fig. 9.2b) and the accompanying expression

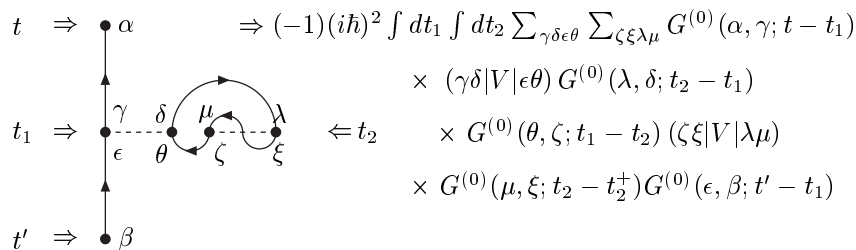


Fig. 9.11 Diagram V2f

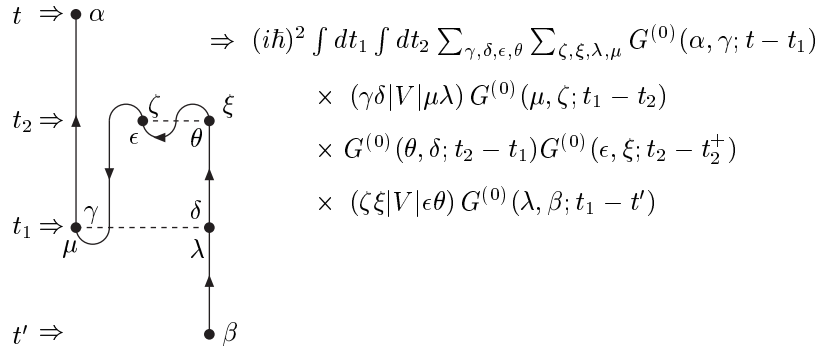


Fig. 9.12 Diagram V2g

is given in Eq. (9.45). In second order, one encounters the contribution to Eq. (9.54) of the form

$$G^{(2)}(\alpha, \beta; t - t') = -\frac{i}{\hbar} \left( \frac{-i}{\hbar} \right)^2 \frac{1}{2!} \int dt_1 \int dt_2 \times \langle \Phi_0^A | \mathcal{T} [\hat{H}_1(t_1) \hat{H}_1(t_2) a_\alpha(t) a_\beta^\dagger(t')] | \Phi_0^A \rangle_{connected}. \quad (9.56)$$

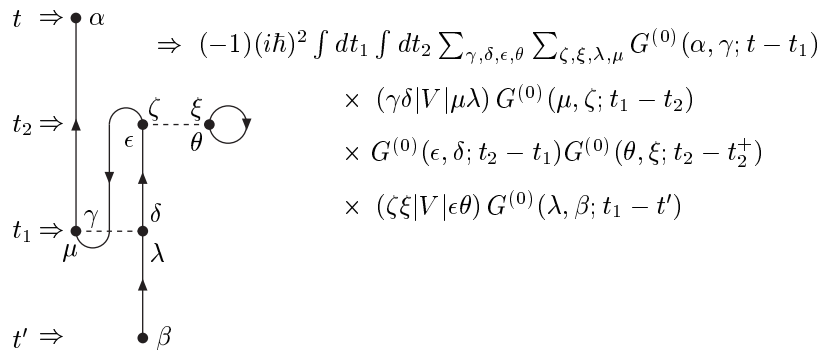


Fig. 9.13 Diagram V2h

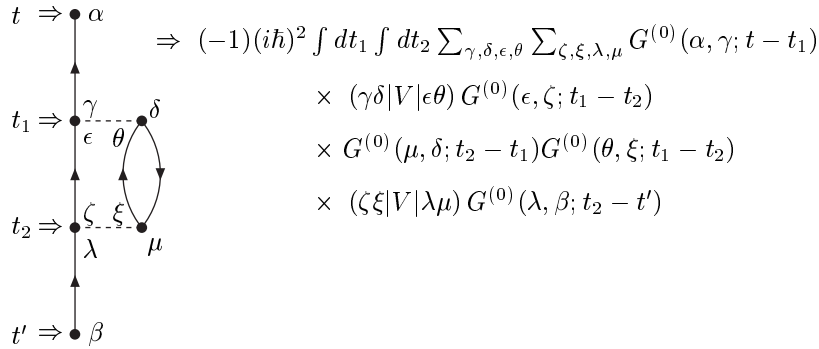


Fig. 9.14 Diagram V2i

Inserting the two contributions to each  $\hat{H}_1$  term requires the evaluation of the following expectation value

$$\begin{aligned} &\Rightarrow \langle \Phi_0^A | \mathcal{T} \left[ \left( \hat{V}(t_1) - \hat{U}(t_1) \right) \left( \hat{V}(t_2) - \hat{U}(t_2) \right) a_\alpha(t) a_\beta^\dagger(t') \right] | \Phi_0^A \rangle_{connected} \\ &= \langle \Phi_0^A | \mathcal{T} \left[ \left( -\hat{U}(t_1) \right) \left( -\hat{U}(t_2) \right) a_\alpha(t) a_\beta^\dagger(t') \right] | \Phi_0^A \rangle_{connected} \\ &+ \langle \Phi_0^A | \mathcal{T} \left[ \hat{V}(t_1) \hat{V}(t_2) a_\alpha(t) a_\beta^\dagger(t') \right] | \Phi_0^A \rangle_{connected} \\ &+ 2 \langle \Phi_0^A | \mathcal{T} \left[ \left( -\hat{U}(t_1) \right) \hat{V}(t_2) a_\alpha(t) a_\beta^\dagger(t') \right] | \Phi_0^A \rangle_{connected}, \quad (9.57) \end{aligned}$$

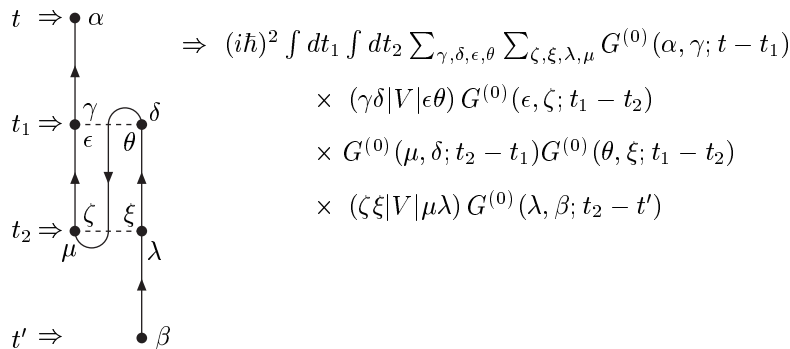


Fig. 9.15 Diagram V2j

where the factor of 2 in the last term originates from relabeling the dummy time integration variables in one of the  $\hat{U}\hat{V}$  products. This factor of two arises also in the other two contributions to Eq. (9.57) resulting from the two identical contributions associated with interchanging the two internal time variables  $t_1$  and  $t_2$ . In second order, one therefore also cancels the corresponding  $1/m!$  term in Eq. (9.54) when  $\hat{U}$  terms are included as in the case when only  $\hat{V}$  terms are considered. This result is also recovered for all higher-order terms. Two additional rules will then have to be added to include these  $\hat{U}$  terms. In particular, when  $k$  such  $\hat{U}$  contributions appear in the diagram one has to

**Rule 6** Label each  $U$  according to

$$\Rightarrow t_i \quad \begin{array}{c} \alpha \\ \bullet \diagdown \diagup \bullet \\ \beta \end{array} \quad \Rightarrow \langle \alpha | U | \beta \rangle$$

**Rule 7** Include a factor  $(-1)^k$  and  $k$  additional propagators  $G^{(0)}$

When  $k$   $\hat{U}$  contributions appear in a diagram, it leads to  $k$  additional contractions representing a factor  $(i\hbar)^k$  since  $\hat{U}$  is a one-body operator and therefore yields only one extra contraction for each  $\hat{U}$ . Together with the factor  $(-1)^k(-i/\hbar)^k$  this yields the factor  $(-1)^k$  quoted in **Rule 7**. It is straightforward to generate the additional diagrams when these  $\hat{U}$  terms are included. Their explicit consideration will be considered in the next chapter where the inclusion of  $\hat{U}$  occurs quite naturally in the analysis presented there. A one-body external field  $\hat{U}_{ext}$  will generate similar terms but doesn't require the factor  $(-1)^k$  in **Rule 7**. It is also wise in this case to select another symbol than the "zigzag" chosen for  $\hat{U}$ .

Another useful diagram strategy may be employed when the relative importance of direct and exchange terms is similar. This happens in the case of nuclear problems for example. It is then convenient to employ the symmetrized version of the two-body interaction as in Eq. (2.46) which involves the combination of direct and exchange matrix elements of the interaction as in Eq. (2.47). One can also obtain the corresponding result by considering the unsymmetrized diagrams as studied in Figs. 9.4 and 9.5 for the first-order contribution and all second-order terms displayed in Figs. 9.6 - 9.15. By relabeling the second term involving  $V$  in Eq. (9.47) and combining the two contributions, one can for example write the first-order contribution as the appropriate contribution is given by Eq. (9.48). Clearly,

when the antisymmetrized version of  $\hat{V}$  is used, one only needs to consider the direct diagram of the first-order contribution shown in Fig. 9.4. The same result is obtained by applying Wick's theorem using the symmetrized version of  $\hat{V}$  (Eq. (2.46)) and applying appropriate relabeling of dummy summation variables. In second order, one can add the first four terms shown in Figs. 9.6 - 9.9 accordingly, by replacing in the expression for diagram *V2a* the two matrix elements of  $V$  by the antisymmetrized terms and only keeping the diagram in Fig. 9.6. Similarly, one can collect the next four terms (Figs. 9.10 - 9.13) of the unsymmetric version and use the corresponding symmetrized matrix elements in the expression for diagram *V2e* while keeping only the diagram (Fig. 9.10). The last two second-order diagrams shown in Figs. 9.14 and 9.15 can also be combined but require a factor of  $1/2$  to get the correct expression. These changes lead to a modified and a new diagram rule when antisymmetrized matrix elements of the interaction are used.

**Rule 1'** Draw only all topologically distinct and connected direct diagrams with  $m$  horizontal interaction lines for  $V$  (dashed) and  $2m + 1$  directed (using arrows) Green's functions  $G^{(0)}$

**Rule 8** Include a factor  $1/2$  for each pair of equivalent lines, where equivalent lines both begin from the same interaction and end at another interaction

The notion of equivalent lines introduced in **Rule 8** originates from the restriction encountered when a pair of lines start and end at the same interaction leading to only two diagrams of the type *V2i* and *V2j* whereas four diagrams occur of the type *V2a-V2d* and *V2e-V2h*, respectively. This feature also occurs in higher order terms resulting in the new rule **Rule 8** when the symmetrized version of the diagrams is employed. As discussed above, certain parts of higher order diagrams contain expressions that correspond exactly to lower order terms. This feature will be very helpful in resumming contributions to the perturbation expansion of the sp propagator. A systematic presentation of this procedure is pursued in Ch. 10.

### 9.5.2 *Energy formulation*

For formal manipulations and the development of the perturbation expansion it has been very useful to employ the time formulation for the propagator. However, as already demonstrated in Ch. 7, for practical results

it is almost always preferable to use the energy formulation. The relevant Fourier transform has already been given in Eq. (8.9) leading to the important Lehmann representation of the sp propagator. A corresponding Fourier transform can then be performed on all the contributions in perturbation theory to Eq. (9.54). It is therefore clear that one may construct a similar diagrammatic framework in the energy formulation. For the non-interacting propagator one can use Eq.(8.35) or directly Fourier transform  $G^{(0)}(\alpha, \beta; t - t')$  according to

$$\begin{aligned} G^{(0)}(\alpha, \beta; E) &= \int_{-\infty}^{\infty} d(t - t') e^{\frac{i}{\hbar} E(t - t')} G^{(0)}(\alpha, \beta; t - t') \\ &= \delta_{\alpha, \beta} \left\{ \frac{\theta(\alpha - F)}{E - \varepsilon_{\alpha} + i\eta} + \frac{\theta(F - \alpha)}{E - \varepsilon_{\alpha} - i\eta} \right\}. \end{aligned} \quad (9.58)$$

While the results of Eq. (9.43) were obtained with the integration limits  $-\infty(1 - i\eta)$  and  $\infty(1 - i\eta)$ , one may convince oneself that employing the integral representation of the step function as given by Eq. (8.9) already removes the unwanted contributions when the difference between the time limits approaches  $\infty$  as discussed in [Mattuck (1992)]. For this reason one can use the integration limits given in Eq. (9.58). While it is possible to Fourier transform each contribution directly, a useful strategy may be to consider the inverse transform for each of the time-dependent unperturbed propagators in each of the terms contributing to the perturbation expansion. This inverse transform is given by

$$G^{(0)}(\alpha, \beta; \tau) = \int_{-\infty}^{\infty} \frac{dE}{2\pi\hbar} e^{-iE\tau/\hbar} G^{(0)}(\alpha, \beta; E). \quad (9.59)$$

Inserting Eq. (9.58) into Eq. (9.59) yields the proper expression for the non-interacting propagator in the time formulation given by Eq. (8.32). In order to obtain this result, one has to extend the energy integral in Eq. (9.59) to complex contour integrals in the lower half (for the particle part of the propagator) and upper half (for the hole part). Application of the residue theorem then yields the correct result. A special case occurs for the noninteracting propagators with equal time arguments. In that case, one has

$$\begin{aligned} G^{(0)}(\alpha, \beta; t - t^+) &= \int_{-\infty}^{\infty} \frac{dE}{2\pi\hbar} e^{-iE0^-/\hbar} G^{(0)}(\alpha, \beta; E) \\ &= \int_{C_{\uparrow}} \frac{dE}{2\pi\hbar} G^{(0)}(\alpha, \beta; E), \end{aligned} \quad (9.60)$$

where the symbol  $C \uparrow$  indicates a contour integral involving the real axis and closed in the upper half plane. In fact, the presence of the  $0^-$  in the first line of Eq. (9.60) forces the contour to be closed only in the upper half of the complex energy plane and, therefore, picks up only the contribution of the hole part.

With these preliminary consideration it is now possible to Fourier transform each expression corresponding to the diagrams in the time formulation thereby obtaining corresponding diagrams in the energy formulation. Subsequently expressing each unperturbed propagator in each of these expressions either according to Eq. (9.59) or (9.60), whichever is appropriate, one arrives at a result in which all the time integrations can be performed without any difficulty. As an example consider the Fourier transform of the expression for the first-order contribution given by Eq. (9.48) and Fig. 9.4 (when using the symmetrized convention)

$$\begin{aligned}
G_V^{(1)}(\alpha, \beta; E) &= \int_{-\infty}^{\infty} d(t-t') e^{\frac{i}{\hbar} E(t-t')} G_V^{(1)}(\alpha, \beta; t-t') \\
&= -i\hbar \int_{-\infty}^{\infty} d(t-t') e^{\frac{i}{\hbar} E(t-t')} \int_{-\infty}^{\infty} dt_1 \sum_{\gamma\delta\epsilon\theta} \langle \gamma\delta | V | \epsilon\theta \rangle \\
&\quad \times \left\{ \int_{-\infty}^{\infty} \frac{dE_1}{2\pi\hbar} e^{-iE_1(t-t_1)/\hbar} G^{(0)}(\alpha, \gamma; E_1) \right\} \\
&\quad \times \left\{ \int_{C\uparrow} \frac{dE'}{2\pi\hbar} G^{(0)}(\theta, \delta; E') \right\} \\
&\quad \times \left\{ \int_{-\infty}^{\infty} \frac{dE_2}{2\pi\hbar} e^{-iE_2(t_1-t')/\hbar} G^{(0)}(\epsilon, \beta; E_2) \right\} \\
&= -i \sum_{\gamma\delta\epsilon\theta} \langle \gamma\delta | V | \epsilon\theta \rangle G^{(0)}(\alpha, \gamma; E) \\
&\quad \times \left\{ \int_{C\uparrow} \frac{dE'}{2\pi} G^{(0)}(\theta, \delta; E') \right\} G^{(0)}(\epsilon, \beta; E), \quad (9.61)
\end{aligned}$$

where the last result is obtained by performing first the integration over  $t_1$  yielding a factor  $\delta(E_1 - E_2)$ , then integrating over  $E_2$ , and, finally, performing the integration over  $t - t'$ . While it is clear that the structure of the diagram remains intact, there are some changes with respect to the labeling. Unperturbed propagators now must be labeled by a single energy. From the above example it also becomes clear that this energy labeling is consistent with energy conservation by each two-body interaction. The arrows of the propagators can therefore also be used to represent the flow

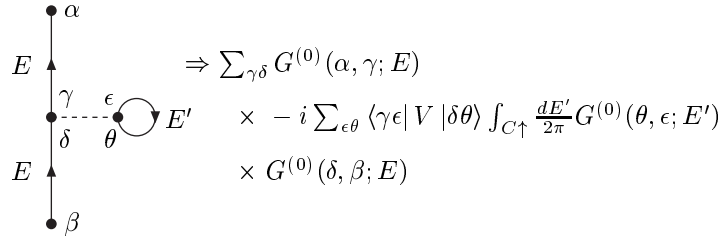


Fig. 9.16 Diagram V1D for the symmetrized version in the energy formulation.

of energy in each diagram such that each interaction has the same energy coming in as flowing out. The diagram representing this first-order contribution in the energy formulation is shown in Fig. 9.16. If only diagrams with  $V$  terms are considered, then for an  $m$ th order diagram one has originally  $m$  time integrations (internal times) plus the external one over  $t - t'$ . Each of these integrals leads to an energy conservation  $\delta$ -function. Replacing each time-dependent  $G^{(0)}$  had already provided  $2m + 1$  factors of  $2\pi\hbar$  in the denominator. From these factors  $m + 1$  are used for time integrals, leaving  $m$  independent energy integrations and a corresponding number of factors of  $2\pi\hbar$  in the denominator (leaving no explicit presence of  $\hbar$  in the final result). When  $U$  terms are included, nothing changes since for  $k$   $U$  terms there are  $k$  extra time integrations and propagators and therefore all factors of  $2\pi\hbar$  cancel and nothing changes. Note that the example illustrated above involved a closed loop. For such loops one simply obtains an independent energy integration (to be closed in the upper half of the corresponding energy plane) which doesn't disturb the energy flow pattern.

The resulting diagram rules mimic closely those obtained for the time formulation. They are given below for the antisymmetrized version and illustrated up to second order in the corresponding diagrams shown in Figs. 9.16 - 9.19.

**Rule 1** Draw all topologically distinct (direct) and connected diagrams with  $m$  horizontal interaction lines for  $V$  (dashed) and  $2m + 1$  directed (using arrows) Green's functions  $G^{(0)}$

**Rule 2** Label external points only with sp quantum numbers, e.g.  $\alpha$  and  $\beta$   
Label each interaction with sp quantum numbers

$$\begin{array}{c} \alpha \\ \bullet \text{---} \bullet \\ \gamma \quad \delta \end{array} \Rightarrow \langle \alpha\beta | V | \gamma\delta \rangle = (\alpha\beta | V | \gamma\delta) - (\alpha\beta | V | \delta\gamma)$$

For each arrow line one writes

$$\begin{array}{c} \bullet \mu \\ | \\ \uparrow E \\ | \\ \bullet \nu \end{array} \Rightarrow G^{(0)}(\mu, \nu; E)$$

but in such a way that energy is conserved for each  $V$

**Rule 3** Sum (integrate) over all internal sp quantum numbers and integrate over all  $m$  internal energies

For each closed loop an independent energy integration occurs over the contour  $C \uparrow$

**Rule 4** Include a factor  $(i/2\pi)^m$  and  $(-1)^F$  where  $F$  is the number of closed fermion loops

**Rule 5** Include a factor of  $1/2$  for each equivalent pair of lines

The diagrams shown in Figs. 9.16 - 9.19 have been purposely accompanied by expressions that emphasize the structure of these diagrams. In particular, it is clear that in the energy formulation all diagrams can be written with an unperturbed propagator  $G^{(0)}(\alpha, \gamma; E)$  at the top and  $G(\delta, \beta; E)$  at the bottom (while summing over  $\gamma$  and  $\delta$ ). A similar structure of the sp

$$\begin{array}{c} \bullet \alpha \\ | \\ \uparrow E \\ \bullet \gamma \\ | \\ \uparrow E \\ \bullet \epsilon \\ | \\ \uparrow E \\ \bullet \zeta \\ | \\ \uparrow E \\ \bullet \delta \\ | \\ \bullet \beta \end{array} \begin{array}{l} \lambda \\ \bullet \text{---} \bullet \\ \theta \quad \theta \end{array} \begin{array}{l} \Rightarrow \sum_{\gamma\delta} G^{(0)}(\alpha, \gamma; E) \\ \times (-1)^2 i^2 \sum_{\epsilon, \zeta} \sum_{\lambda, \theta} \int_{C \uparrow} \frac{dE'}{2\pi} \langle \gamma\lambda | V | \epsilon\theta \rangle G^{(0)}(\theta, \lambda; E') \\ \times G^{(0)}(\epsilon, \zeta; E) \sum_{\xi, \mu} \int_{C \uparrow} \frac{dE''}{2\pi} \langle \zeta\xi | V | \delta\mu \rangle G^{(0)}(\mu, \xi; E'') \\ \times G^{(0)}(\delta, \beta; E) \end{array}$$

Fig. 9.17 Diagram V2a in the symmetrized version of the energy formulation

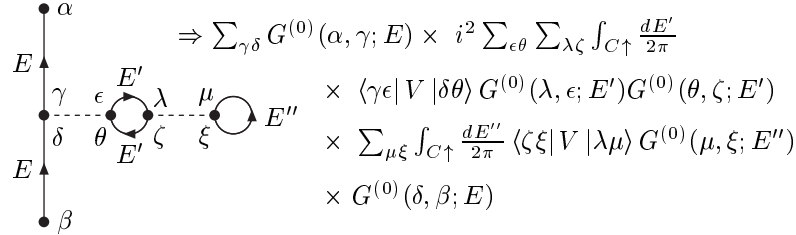


Fig. 9.18 Diagram V2e for the symmetrized case in the energy formulation

propagator was encountered in Ch. 7 in the case of the one-body problem. This structure will be employed in Ch. 10 to organize the expansion in a similar way as in Ch. 7.

Sofar only terms involving the two-body interaction are included. Additional diagrams with  $U$  terms can be easily included by noting that on account of their one-body character, the energy associated with the incoming propagator must be equal to that of the outgoing one. Similar statements (and rules) hold when an auxiliary potential is included. When in a diagram  $k$   $U$  contributions are involved one has to add to the above rules the following ones similar to the case of the time formulation.

**Rule 6** Label each  $U$  according to

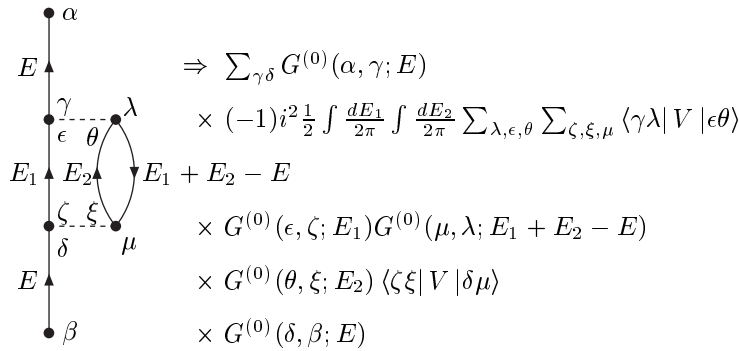


Fig. 9.19 Diagram V2i for the symmetrized version in the energy formulation

$$\begin{array}{c} \alpha \\ \bullet \\ \diagup \\ \diagdown \\ \bullet \\ \beta \end{array} \Rightarrow \langle \alpha | U | \beta \rangle$$

**Rule 7** Include a factor  $(-1)^k$  and  $k$  additional propagators  $G^{(0)}$

By now it should be clear how to generate the rules for the unsymmetrized version of the diagrams in the energy formulation.

## 9.6 Exercises

- (1) Evaluate the expectation value of the first-order contribution to the numerator in Eq. (9.17) for the  $\hat{U}$  term for the time-orderings not considered here. Construct the corresponding time-ordered diagrams in all these cases.
- (2) Evaluate the expectation value of the first-order contribution to the numerator in Eq. (9.17) for the  $\hat{V}$  term for all possible time-orderings. Construct the corresponding time-ordered diagrams in all these cases.
- (3) Construct all Feynman diagrams in third order involving only contributions of the two-body interaction and write down the corresponding expressions from the diagram rules (in the unsymmetrized version).
- (4) Same as the previous problem but now in the energy formulation and the symmetrized version.

